RIGA TECHNICAL UNIVERSITY
Faculty of Mechanical Engineering, Transport and Aeronautics
Institute of Aeronautics

Yevhen HARBUZ
Doctoral Student of the Study Programme “Transport”

AVIATION MATERIAL AND CONSTRUCTION FATIGUE DAMAGE ASSESSMENT ON THE BASIS OF ACOUSTIC EMISSION SIGNALS

Field: Mechanical Engineering

Subfield: Measurement Instrumentation and Meteorology

Summary of Doctoral Thesis

Scientific supervisor
Dr.habil. sc.ing., Professor
A. URBAHS

RTU Press

Riga 2015

Harbuz Y. Aviation Material and Construction Fatigue Damage Assessment on the Basis of Acoustic Emission Signals. Summary of Doctoral Thesis. — R.: RTU Press, 2015.— 33 p.

Printed according to the Resolution of the Institute of Aeronautics, as of 2nd April 2015, Minutes No. 02/2015

The present research has been supported by the European Social Fund within the project "Support for the Implementation of Doctoral Studies at Riga Technical University".

ISBN 978-9934-10-739-9

DOCTORAL THESIS PROPOSED TO RIGA TECHNICAL UNIVERSITY FOR THE PROMOTION TO THE SCIENTIFIC DEGREE OF DOCTOR OF ENGINEERING SCIENCES

To be granted the scientific degree of Doctor of Engineering Sciences, the present Doctoral Thesis has been submitted for the defence at the open meeting of RTU Promotion Council 13th October 2015, at 1.00 p.m. at Riga Technical University, the Faculty of Mechanical Engineering, Transport and Aeronautics, 6 Ezermalas Street, Room 405.

OFFICIAL REVIEWERS

Prof., *Dr.sc.ing.* Juris Krizbergs
Riga Technical University, Latvia

Prof., *Dr.habil.sc.ing.* Valdis Priednieks
Latvian Maritime Academy, Latvia

Prof., *Dr.habil.sc.ing.* Jonas Stankūnas
Vilnius Gediminas Technical University,
Director of Antanas Gustaitis` Aviation Institute, Lithuania

DECLARATION OF ACADEMIC INTEGRITY

I hereby declare that the Doctoral Thesis submitted for the review to Riga Technical University for the promotion to the scientific degree of Doctor of Engineering Sciences is my own and does not contain any unacknowledged material from any source. I confirm that this Thesis has not been submitted to any other university for the promotion to other scientific degree.

Yevhen Harbuz …………………………….(signature)

Date: ………………………

The Doctoral Thesis has been written in Latvian; it contains introduction, 5 chapters, conclusion, bibliography with 148 reference sources, and 6 appendices. It has been illustrated by 114 figures. The volume of the present Doctoral Thesis is 174 pages.

CONTENTS

GENERAL DESCRIPTION OF THE THESIS

Topicality of the Research

A machinery (vehicle, including, air ships, space devices and others) resource is usually determined on the basis of the results of the stand fatigue test. “Weakest” design elements limiting the resources of the entire object as a whole are determined during the stand tests; determining cell survivability and viability. Furthermore, one of the most important and most difficult problems is the need to discover defects at an early stage that have emerged during the testing process of the construction material. An important problem is the kinetic control of crack propagation.

The following traditional non-destructive test methods are used for control and diagnostics in fatigue test: visual optical, ultrasonic, eddy current, powder magnets as well as capillary method (colour and luminescence). All of these methods have limitations related to the fact that fatigue cracks usually occur in various parts of the joints, which in most cases are difficult or even impossible to access without disrupting the connection. They cannot be used to control defects, which occur within the elements of the object, i.e., traditional method is effective if it is possible to disassemble the construction. In addition, these methods are very time-consuming because of the need to scan virtually the entire surface of the object.

One of the methods without most of the drawbacks mentioned herein is the acoustic emission (AE) method. This method is based on the elastic wave (wave voltage) emergence and spread process analysis, which causes changes in the structure of the rigid body at different loads. Since these changes are related mainly to the material decay processes, it is possible to identify both the emergence and development of various defects. Furthermore, the AE method enables the performance of an integrated object damage assessment and determination of defect locations.

Aviation construction damage control with the acoustic emission method during the stand testing process will allow discovering dangerous defects in the testing process, such as fatigue fracture at an early stage, evaluating the durability of the construction and predicting its resources during the process of use.

Aims and Tasks of the Research

The aim of the Doctoral Thesis is to research the collapse mechanism of aviation metallic and composite structures, as well as to develop damage assessment methodologies in the resource tests based on AE signal measurements.

To achieve this aim, it is necessary to solve the following tasks:

1. To develop a mathematical model that describes an assessment mechanism of metallic material fatigue damage based on acoustic emission measurement data.
2. To investigate the aviation structures of metallic material fatigue failure mechanism in stand tests and to develop assessment criteria for metallic material fatigue damage based on acoustic emission signal measurements.
3. To research the aviation composite collapse mechanism and to develop a damage degree assessment criterion of composite using the AE signal data registration.
4. To examine the collapse mechanism of real composite structures and to test the efficiency of damage assessment methodology using AE measurement data.

Research Methods

In the present research, the following research methods have been used:

1) Acoustic signal measurements with AF-15 and POCKET AE-2 measuring aperture according to Euro Standard EN 1330-9:2000 “Terms. Acoustic Emission Conceptions” guidelines.
2) The computer programs AEWin, Catman and Akusto to process the AE signal measurement results.
3) The computer program EXCEL to process the experimental results.
4) Probability theory and static method for error (uncertainty) analyses.

Object of the Research

Required data have been obtained by testing a sample group of composite materials as well as on full-scale structures — an airplane wing aileron, which is made out of composite material. Part of the results of metallic materials is devoted to the research of the material damage of mechanism on an airplane chassis example.

The experimental part took place in “AVIATEST LNK” base, experimental centre of Riga, testing aviation materials and full-scale structures.

Scientific Novelty of the Doctoral Thesis and Main Results of the Research

The innovative solutions created as a result of the Doctoral Thesis:

1. A mathematical model has been created for evaluating the mechanism of fatigue damage of the material based on measurement data. The model takes into account fatigue damage accumulation order, including material plastic deformation as well as micro and macro fracture formation and spread.
2. A new quantitative assessment method of metal construction fatigue damage area has been proposed based on AE measurements.
3. New criteria for the test to determine object residual strength — load value has been proposed, which corresponds to object collapse beginning moment, which is registered as a result of acoustic emission measurements.
4. Composite construction damage process assessment method has been proposed on the basis of measurement data.

These innovative solutions contribute to machine science and production integration as well as to research result introduction in accordance with the priorities set out by the country for the scientific direction — “Innovative Materials and Technologies”.

Practical Use of Research Results

The developed aviation and structural damage assessment method that can be used for both scientific and practical purposes, performing fatigue and residual stand strength testing, is useful not only for aviation equipment but also in other engineering areas: automotive, rail and sea transportation, spacecraft etc. The residual strength criteria have emerged in other potentially dangerous engineering operation formations, for example, nuclear fuel storage facilities, pressure tanks etc.

Thesis Statements to Be Defended

The author in the theses defends:

1. Mathematical mode, which describes metallic material fatigue damage assessment mechanism, based on acoustic emission measurement data.
2. Aviation construction made of metallic materials, fatigue damage assessment criteria based on acoustic emission control.

3. Aviation composite damage degree assessment method.
4. Real airship construction out of composite material damage assessment experimental results.

The Approbation of the Research Results

Results of the research have been reported in 11 international scientific conferences:

1. The 15th International Conference "Mechanika – 2010", April 8–9, 2010, Kaunas, Lithuania.
2. The 14th International Conference "TRANSPORT MEANS 2010", October 21–22, 2010, Kaunas, Lithuania.
3. The 2nd International Symposium "Space & Global Security of Humanity", 5–9 July, 2010, Riga, Latvia.
4. RTU 51st International Scientific Conference, October 11–12, 2010, Riga, Latvia.
5. The 8th International Conference "AES-ATEMA'2011", July 18–20, 2011, Riga, Latvia.
6. The 16th International Conference "Mechanika – 2011", April 8–9, 2011, Kaunas, Lithuania.
7. The 15th International Conference "TRANSPORT MEANS 2011", October 21–22, 2011, Kaunas, Lithuania.
8. The 17th International Conference "Mechanika – 2012", April 12–13, 2012, Kaunas, Lithuania.
9. The 16th International Conference "TRANSPORT MEANS 2012", October 25–26, 2012, Kaunas, Lithuania.
10. International Conference "Intelligent Transport Systems 2012", June 18–20, 2012, Riga, Latvia.
11. The 20th International Conference "Mechanika – 2015", April 23–24, 2015, Kaunas, Lithuania.

Papers

The research results have been published in 9 scientific papers and have received 3 patents:

1. Urbahs A., Banovs M., Harbuz Y., Doroshko S., Turko V. Acoustic emission diagnostics of fatigue crack development during undercarriage bench. Proceedings of the 15th International Conference "Mechanika – 2010", Kaunas, Lithuania, KTU, April 8–9, 2010, pp. 450–454.
2. Urbahs A., Banovs M., Harbuz Y., Turko V., Feščuks Y., Hodos N. Estimation of mechanical properties of the anisotropic reinforced plastics with application of the method of acoustic emission. Transport and Telecommunication, Vol. 5, No. 2, 2010, pp. 68–75, SCOPUS.
3. Nasibulins A., Harbuz Y., Doroško S. Acoustic emission characteristics of fatigue crack development in a pitch control arm of helicopter lifting propeller blades. Proceedings of the 14th International Conference "Transport Means – 2010", Kaunas, Lithuania, KTU, October 21–22, 2010, pp. 49–52, SCOPUS.
4. Urbahs A., Banovs M., Harbuz Y., Turko V., Feščuks Y., Hodos N. Investigation of Mechanical Properties of Composite Materials Using the Method of Acoustic

Emission. Proceedings of the 16th International Conference “Mechanika – 2011”, Kaunas, Lithuania, KTU, April 8–9, 2011, pp. 306–310.

5. Urbahs A., Banovs M., Harbuz Y., Feščuks Y., Čepusovs A. Evaluation of residual strength of aircraft aileron construction. Proceedings of the 8th International Conference “AES-ATEMA’2011”, Riga, Latvia, July 18–20, 2011, pp. 29–33. SCOPUS.
6. Urbahs A., Banovs M., Harbuz Y., Feščuks Y., Sologubovs J. Evaluations of degree of damage and probability of forecasting of destructing load in anisotropic composites by means of acoustic emission in materials under static loading, Proceedings of the 15th International Conference “Transport Means – 2011”, Kaunas, Lithuania, KTU, October 21–22, 2010, pp. 270–273, SCOPUS.
7. Doroško S., Harbuz Y. Acoustic emission analysis of fatigue crack development. Proceedings of the 17th International Conference “Mechanika – 2012”, Kaunas, Lithuania, KTU, April 12–13, 2012, pp. 73–76.
8. Harbuz Y., Chepusov A. Methods of acoustic emission diagnostics of pre-destruction state. Proceedings of the 16th International Conference “Transport Means – 2012”, Kaunas, Lithuania, KTU, October 25–26, 2010, pp. 228–231, SCOPUS.
9. Urbahs A., Harbuz Y., Urbaha J. Evaluating of Damageability of Materials at Fatigue Loading Based on Signals of Acoustic Emission. Proceedings of the 20th International Conference “Mechanika – 2015”, Kaunas, Lithuania, KTU, April 23–24, 2015, pp. 257–261.

Patents:

1. Doroško S., Harbuz Y. Method of detection of the crack size in fatigue tests, LR Patent No. 14488, 2012.
2. Doroško S., Harbuz Y. Method of limit load determination during residual strength testing, LR Patent No. 14531, 2012.
3. Doroško S., Harbuz Y. Method of determination of composite material destruction type, LR Patent No. 14585, 2012.

The results of the Doctoral Thesis have been used in two scientific projects:

1. ERAF project No. 2DP/2.1.1.1.0/10/APIA/SEDA/135 “Development of Industrial Technology Prototype, Nanostructured Multicomponent Ion-plasma Wear-resistant Coatings” since 2010.
2. ERAF project No. 2DP/2.1.1.1.0/10/APIA/SEDA/070 “Autonomous Aviation Complex Development and Development of Aircraft Industrial Prototypes for the Solution of Latvian Economy Tasks.

Structure and Contents of the Doctoral Thesis

The Doctoral Thesis has been written in Latvian; it contains introduction, 5 chapters, conclusion, bibliography with 148 reference sources, and 6 appendices. It has been illustrated by 114 figures. The volume of the Doctoral Thesis is 174 pages.

CONTENTS OF THE DOCTORAL THESIS

Introduction

The following traditional non-destructive test methods have been used for control and diagnostics in fatigue test: visual optical, ultrasonic, eddy current, powder magnets as well as capillary method (colour and luminescence). All of these methods have limitations and disadvantages. One of the methods without most of the drawbacks mentioned herein is the acoustic emission (AE) method.

Chapter 1. Analysis of the Methods of Evaluating the Technical Condition and Residual Strength of Aviation Constructions

The first chapter of the Doctoral Thesis deals with aero construction remaining resource assessment capabilities which are made out of metallic and composite materials. Defect analyses of material used in aeromechanics have been carried out.

Lately, composites are increasingly used in the construction of aero constructions that have a number of unique properties, which also determines that composites are to be chosen instead of metallic materials.

To detect different defects in aviation, different types of detection techniques have been used. The most common is non-destructible control method (NCM); it allows detecting defect in time of exploitation, between flights or at the time of monitoring of all components and assemblies while performing planned maintenance. But to study gliders constructions main nodes and technical conditions of motor units in depth it required to be disassembled.

Solving this problem, as well as a series of other problems that are related to the Thesis, finance and time loss caused by doing unnecessary implement and mechanical disassembly — assembly of their preparation for diagnosis, etc. related work, could be done using the acoustic emission (AE) method. This method has many advantages compared to other NCM.

Chapter 2. Material Damage Assessment in Load Cycling Process Based on Acoustic Emission Signal Measurement Data

2.1. Analysis of the Nature of Sources of Acoustic Emission and Mechanism of Fatigue Failure of Metallic Materials

The analysis of signals of AE sources allows us to identify the origin and development processes of material defects at different stages of fatigue loading. The AE source is a field of material, in which the structure dynamic restructuring is carried out, accompanying AE [36].

According to the results of a number of studies carried out, including the ones by the author of the Doctoral Thesis [14,17,19,26,36], it has been found that the development of a fatigue crack occurs in several stages. There are various processes associated with the transformation of the internal material defects (dislocations) at the first stage (Fig. 1): development or annihilation of dislocations, their movement, shape change, etc. Some energy accumulates in the material as a result of the loading force work. The 2nd stage is appearance of a micro crack (free surface in continuity of the material), followed by the release of energy. The most common is a variant, when initially some micro cracks occur, which are merging into a single crack at the end of the phase. The 3rd stage — stop of the growth of the main crack and re-accumulation of energy (there are shifts in the individual load cycles and, therefore, the slow crack growth in these cycles occurs at this stage). The stored energy is released at some point: this energy provides operation of the crack growth, which occurs at each loading cycle — this is stage 4. Then the new stop or slow crack growth occurs. Stages 3 and 4 can be repeated several times (stages 5 and 6 in Fig. 1). The final stage (stage 7) is a catastrophic crack growth, ending with the destruction of the test object.

Such behaviour of AE is typical of most metallic constructional materials that possess both certain brittleness and significant plastic properties.

Thus, if one registers only the AE components from plastic deformation and crack jumps, the following principal features of the mechanism of crack propagation in metallic materials can be noted:

- Development of a fatigue crack occurs in several stages.
- The crack growth has a discrete character (at the same time the crack growth does not occur in those cycles, where there is no release of energy. As a result, all load cycles can be divided into active (with AE signals) and passive (without AE signals).
- Simple pulses or pulse bursts can occur in active cycles. These features reflect the uneven development of a fatigue crack and possibility of few of its jumps in the region of the maximum load.
- The crack growth is determined by the work done for its formation (energy released in the process of its growth), i.e., the size of the crack depends on the magnitude of this energy. The energy value may be determined based on the results of measurements of AE.

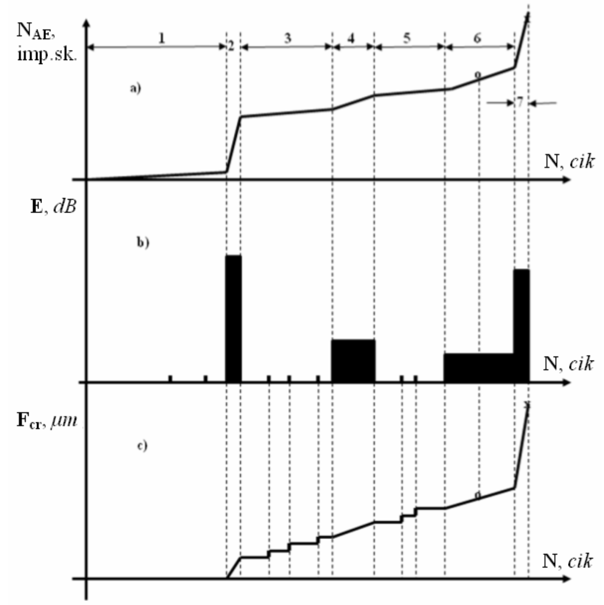

Fig. 1. The process schemes of energy release:
a) change of total counting of AE N_{AE} during cyclic loading; b) release of energy E, expended for the work in providing the crack growth; c) change in the crack growth in accordance with change of energy E

These features underlay the proposed model of estimation of the material damageability under fatigue loading on the basis of measurements of acoustic emission signals [25].

2.2. Simulation of the Damage of Materials during Fatigue Loading Based on the Measurements of the Acoustic Emission Signals

The impulse sequence of discrete AE within a single loading cycle can be characterised by the following basic parameters [5,6,17,19,21,22,24,25,26,36]:

- The number of AE pulses in the cycle n of loading N_{in}, imp;

- Amplitude particular pulse I of AE in the cycle n of loading A_{in}, dB;
- Energy of AE signals in the n-th cycle of loading E_n, dB.

In the case of an uninterrupted AE instead of N_{in} to evaluate the damage of the material total AE N_{AEn} (imp.sk.) should be used in the cycle n at the selected level of discrimination (restricted value of destruction) signal [5,6,17,19,21,22,24,25,26,36].

Source 1: plastic deformation of the material

To simplify the theoretical definition of connections between the parameters of AE signals and sources of fatigue damage in the material let us assume the following hypothesis [36]: the total of AE during the plastic deformation of the material, under other conditions being equal, is proportional to the plastically deformable volume

In that case:

$$N^*_{AEn} = N^*_{AE0} \cdot V \tag{2.1}$$

N^*_{AEn} — the total score of AE in the loading cycle n during plastic deformation of the material, imp.sk.;

N^*_{AE0} — the score of AE signals generated by the local unit of plastically deformable volume **V** of the material, imp.sk.·mm^2.

Condition (9.1) can be written in differential form, defining the counting rate:

$$\dot{N}^*_{AEn} = \frac{dN^*_{AEn}}{dt} = N^*_{AE0\varepsilon} \cdot \dot{\varepsilon} \cdot V + N^*_{AE0} \frac{dV}{dt} \tag{2.2}$$

where $N^*_{AE0\varepsilon} = \frac{dN^*_{AE0}}{d\varepsilon}$ — the total score of AE caused by the change in volume of the plastic deformation;

$\dot{\varepsilon} = \frac{d\varepsilon}{dt}$ — the speed of deforming the local unit of the plastically deformable material volume.

In that case, based on data from the AE parameters it is possible to evaluate the local volumes of plastically deformable material **V**.

Source 2: the growth of a fatigue crack

An elementary example of crack enlargement l is to increase its length by a small amount dl. This process is accompanied by the emission signal AE of high amplitude. Estimate of the amplitude of the pulse is held using the known ratio, which allows determining the movement of the particles of the material in the vicinity of a crack in a generalised form [34,35,36]:

$$\delta_{ijn} = \frac{K_j}{I} \sqrt{\frac{r}{2\pi}} \varphi_{ijn}(\theta, \mu, \tilde{r}), \ (\mu\text{m}) \tag{2.3}$$

where the stress intensity coefficient

$$K_j = P_j \sqrt{\pi l} Y_j(\lambda) \tag{2.4}$$

In formulas (2.3) and (2.4):

r,θ — the polar coordinates of the researched point of material in relation to the crack tip;

$\varphi_{ijn}(\theta,\mu,r)$ — dimensionless function of angle θ, Poisson's ratio μ, and relative coordinates $\bar{r} = \frac{r}{h}$;

h — the thickness of the wall of the construction with crack,
J — shear modulus,
p_j — external component of the specific load corresponding to the type of fracture;
$Y_j(\lambda)$ — dimensionless correction function of relative crack length,
$\lambda = \frac{l}{L}$ — the ratio of the absolute crack length l (μm) to the characteristic size L (μm) design (length or width — depending on the crack).

Function $Y_j(\lambda)$ depends on several factors such as a crack, its configuration and orientation with respect to the coordinate axes, the geometric parameters of the object, and the load characteristics, etc.

Assuming that the amplitude of the AE signals is proportional to the corresponding increment movements in the vicinity of the crack tip $A_{ijn}=\delta_{ijn}$, we obtain that for the case of linear increase in crack length:

$$\Delta A_{ijn} = \frac{\partial \delta_{ijn}}{\partial l} dl \qquad (2.5)$$

In this case an increase in the linear size of the fatigue crack is possible to control, registering both amplitude and the parameters of the total energy bill and AE signals.

Furthermore, in formula (2.4) of the external load component allows evaluating fracture also incremented by the values of the load, given that cyclic loading increment dl localized cracks in the vicinity of the maximum load, i.e., $p_j = p_{jmax}$. This makes it possible to estimate the magnitude of fatigue damage as structural material in terms of AE, and in terms of load parameters.

Parameter S_{cr} is determined according to the formula:

$$S_{cr} = \frac{N_{AE2} - N_{AE1}}{(N_2 - N_1) \cdot P_{\max} \cdot A} \qquad (2.6)$$

S_{cr} — damaged area value, mm^2;
N_{AE1}, N_{AE2} — AE summary number, imp.sk;
N_1, N_2 — load cycle number, cik;
P_{max} — maximum load, kN;
A — integral parameter, which takes AE parameter cycles into account, as well as outer load and damage size, $\frac{imp.sk.}{cik \cdot k\dot{N} \cdot mm^2}$

Parameter A can be determined experimentally, testing samples until they completely collapse, if one knows damaged area value (S_{cr}) summary AE number (N_{AE1}, N_{AE2}), load cycle number (N_1, N_2) as well as loading condition parameters (P_{max}).

Chapter 3. Methodology of Experimental Research and Applied Equipment

3.1. Characteristics of the Research Objects

The following research objects have been selected:
1. Composite samples;
2. Medium main airplane (MMA) chassis basic frame;
3. Low main airplane (LMA) wing aileron.

3.1.1. Characteristics of Composite Samples

To investigate KM damage mechanism, three groups of samples have been studied; the samples have been made of the same direction oriented composites [Harbuz Y., Urbahs A., Nasibullins A., Banovs M., Feščuks J. etc.]:

- Composite material samples with longitudinally and transversely oriented fibres in relation to the load vector. Samples formed as rectangular plates with the ends fixed in brackets designed to carry out stretch tests until complete sample collapse (Fig. 2, a.)
- Composite materials, which are designed as cross shaped plates and prepared for stretch test until complete sample collapse (Fig. 2, b);
- Composite samples, which are shaped as Maltese cross plates and prepared for stretch test until complete sample collapse (Fig. 2, c).

The samples have been made according to ГОСТ 12019-66, 11262-80 textile backing T-50 (ВМП) – 18, which is made according to ТУ 6-48-5786902-9-88, and a binder 5-211Б ПИ 1.2.266 – 84 total number of layers is seven.

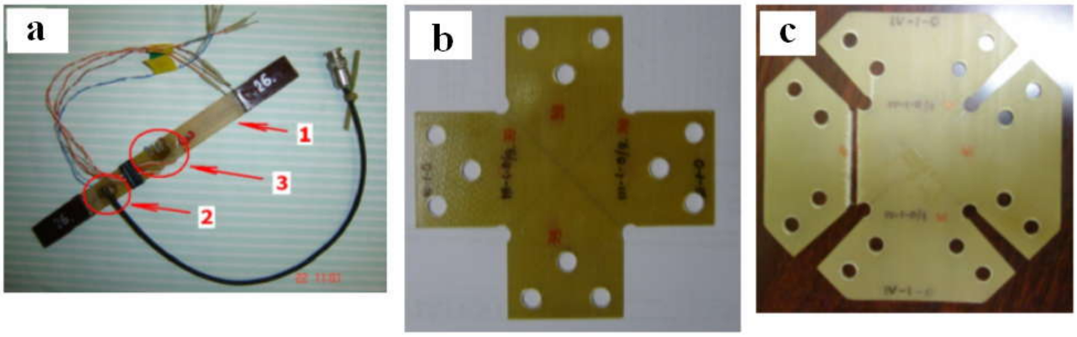

Fig. 2. Overview of composite samples

3.1.2. MMA Design Features of Basic Rack

The most dangerous chassis rack damage is fatigue crack in welds and material that promotes the subsequent collapse of the material. Typically in the fracture voltage occurs at concentration areas — in areas with significant changes in the strength, the wellhead, rounded transitions, complex configuration areas, etc.

Aircraft MMA chassis base frame (Fig. 3) has been selected as the subject of research.

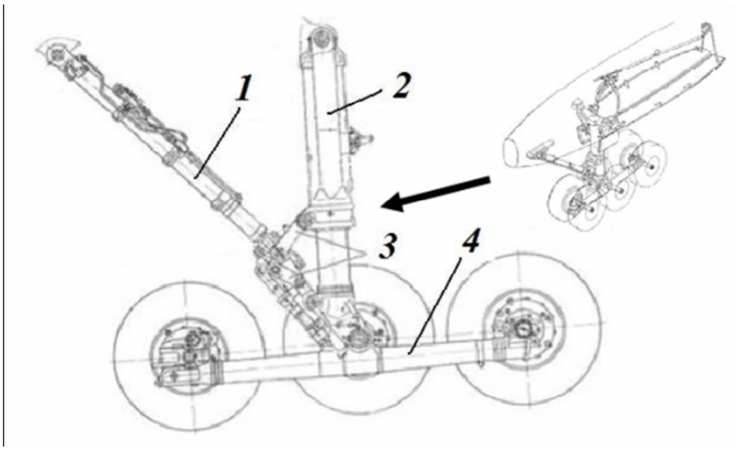

Fig. 3. MMA airplane chassis basic rack component:
1 — inclination cylinder, 2 — amortization base support, 3 — ribbed hinge, 4 — wheel cart

3.1.3. Special Features of Airplane LMA Aileron Construction

In the Doctoral Thesis, aircraft LMA wing aileron (Fig. 4) has been chosen as an object of the research.

The fact that this mechanism has been chosen as the object of the research can be explained by the fact that in the LMA aircraft aileron construction consists of composites.

Figure 5 presents an applicability scheme of a variety of materials from the manufacturing process of this airplane.

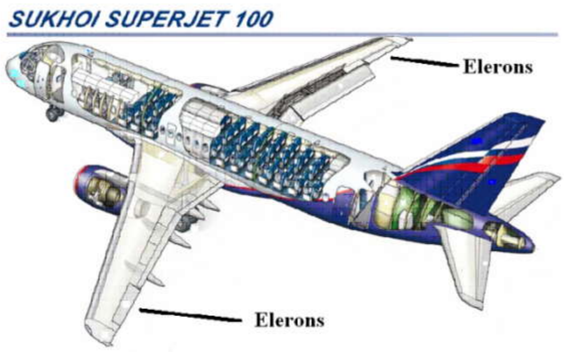

Fig. 4. The studied aileron location scheme on airplane LMA

Fig. 5. The utilitarian scheme of various materials in the production process of LMA aircraft:
blue colour — metal; orange — carbon fibre; yellow — glass fibre

3.2. Methodology of Experimental Studies

3.2.1. Experimental Stand and Methodology of Composite Sample Studies

Composite material tests took place in a thermostatic stand equipped with a hydraulic cylinder and strain gauge system. Under load conditions were put down and controlled with a specially designed "Aviatest" system. The stand is an experimental facility WPM – 2 Germany [17,21,22,23] developed at the laboratory "LNK AVIATEST" (Fig. 6).

Fig. 6. Test stand thermostatic chamber

In the time of testing, it was necessary to maintain temperature conditions in the range of + 22 ... 24 ºC.

Composite sample, which is designed as a rectangular plate with the ends fixed in brackets and sample shaped as Maltese cross plate, test programme predicted that a part of samples will be loaded once until complete collapse, but other samples by programme that expected to be loaded tree times until the level reaches 10 %–30% from collapse pressure and subsequent loading of samples to collapse (Fig. 7).

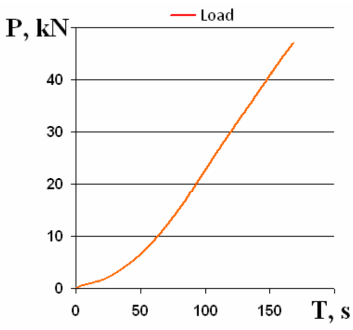

a)

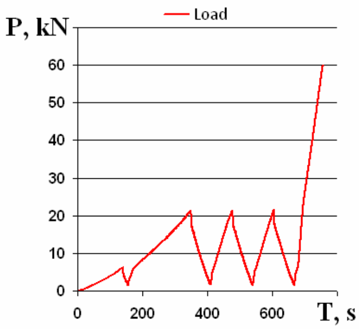

b)

Fig. 7. The sample is formed as a rectangular plate, load conditions of the program for composites with longitudinal fibre orientation against the load condition vector

Each group of KM initial load value corresponded to the following values in the range:

- composites with longitudinal fibre orientation against the load conditions vector — from 20 to 23 kN;
- composites with transversal fibre orientation against the load conditions vector — from 2 to 4 kN;
- cross-shaped KM — from 12 to 15 kN;
- KM Maltese cross-shaped form — from 7 to 10 kN.

AE signal transducers were glued on samples in specially selected areas with cyanoacrylate adhesive with further withstanding of 4–5 minutes.

3.2.2. Airplane MMA Chassis Frame Inspection Stand and Test Methodology

For chassis trial “LNK AVIATEST” stand complex was used.

Load activity impact diagram on the chassis support is shown in Fig. 8.

The chassis fatigue test stand is shown in Fig. 9.

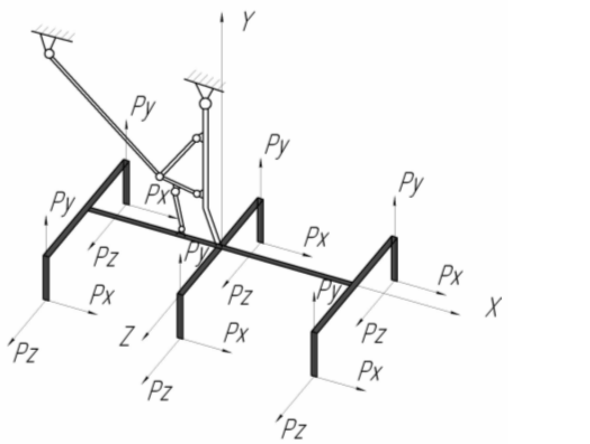

Fig. 8. Load influence scheme on chassis main support

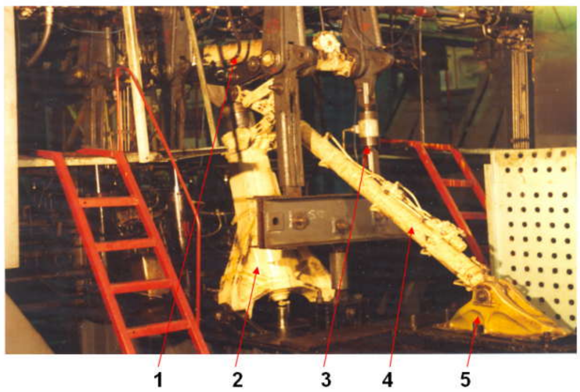

Fig. 9. The overall chassis test stand appearance:
1 — carts; 2 — shock absorber;
3 — loading system hydro cylinder;
4 — stanchion; 5 — bracket

The fatigue test loading program mimicked the chassis standard load of in-flight process. In one loading block one basic loading cycle was mimicked — “take off — landing”. The loading block consists of forces and variable loads, which arise from the following flight modes:

- turns before take-off;
- release of the brakes;
- steering and take off;
- chassis and retraction and release;
- landing;
- turns after landing.

Load values were selected on the basis of measurements, which took place in the factory where the chassis were made and tested, as well as according to the data, which were obtained by running the process. Trials from the concentrator, which was placed on the shock absorber rod inner surface, had to obtain fatigue fracture.

To reduce the time needed for fracture to arise, the following program was selected — loading was carried out by pulsed lateral forces P_z = 0...10.6 tonnes (Fig. 8) with constant vertical load P_y = 45.0 tonnes. Lateral force P_z was added opposite to kerf chosen in such a way as to create a kerf opening.

Real loading parameter measurements showed that minimum lateral load value was $P_{z\ min}$ = 0.1 ton; maximum lateral load was $P_{z\ max}$ = 10.5 tonnes (at the same average value $P_{z\ mid}$ = 5.4 tonnes). Average load period was 50 seconds (trail process varied from 30 to 60 seconds).

After the frame was subjected to the tests of residual strengths (Fig. 10), load was increased gradually (in each of the loading conditions 10 % from calculated collapse load). It collapsed completely under the load, which consisted of 90 % of the calculated. At the same time synchronously with the loading condition changes AE signals were measured.

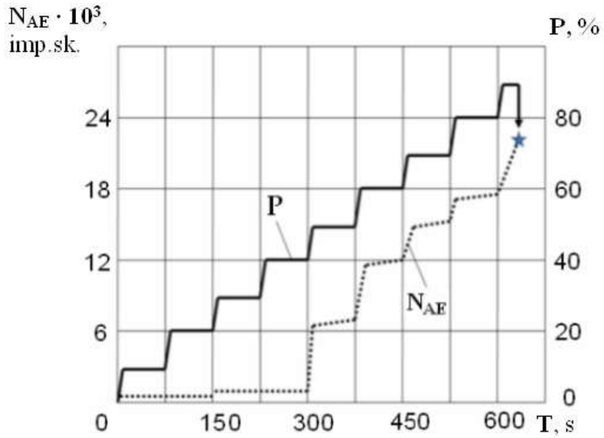

Fig. 10. Summary AE number N_{AE} and load P dependence scheme in time T (— collapse moment)

3.2.3. Aileron Static Test Stand and the Description of Methodology

For aileron test scientific experimental centre of Riga “LNK AVIATES” stand complex was used.

Test stand overview is shown in Fig. 11 [20].

Aileron static test program on an isolated stand moisture saturation condition was developed to calculate and experimentally justify aileron static strength.

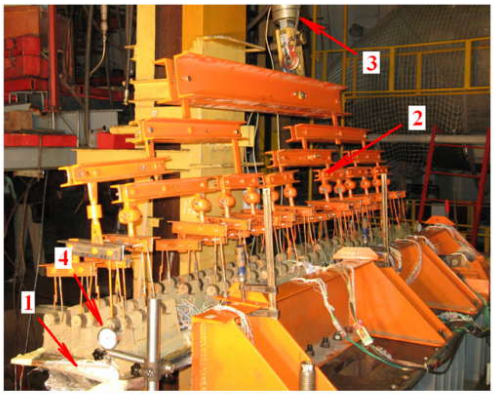

Fig. 11. Aileron view in test stand:
1 — aileron; 2 — loading stand; 3 — loading hydro cylinder; 4 — dial indicator

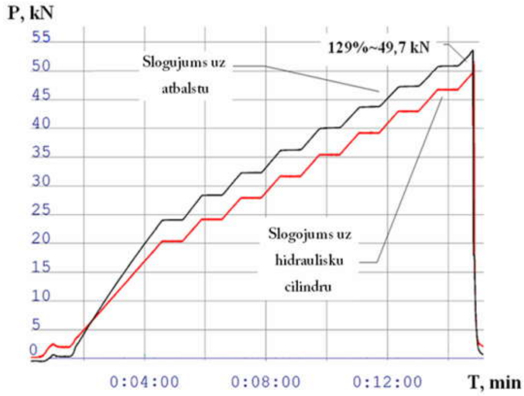

Fig. 12. Aileron load cyclorama in static tests

During the study, the following parameter values were assigned: rear aileron edge was directed towards the bottom by 11.60 corresponding to the flight conditions H = 7560 m attitude with V = 660 km/h, flight mass G = 45880 kg and overload n_y = 1.67; aerodynamic load on aileron in this case is equal to Pp = 3668 kg: mounted external booster (simulator).

Aileron load until collapse cyclorama is shown in Fig. 12.

Aileron moisture saturation was performed in special camera (manufacturer — JEIO TECH).

Moisture saturation program was as follows:

- moisture saturation duration — 2.5 months without interruption;
- temperature — 80 °C;
- moisture — 85 % HR.

3.3. Applied Acoustic Emission Hardware Technical Characteristics

During the test, two AE signal registration and processing complexes were used; they were made using machines AF-15 (Moldova) (Fig. 13) and POCKET AE-2 Physical Acoustics Corporation (PAC), (ASV) (Fig. 14).

Test measuring aperture commutation scheme is shown in Fig. 15.

Fig. 13. Analyser AF–15

Fig. 14. Company’s PAC POCKET AE-2 device

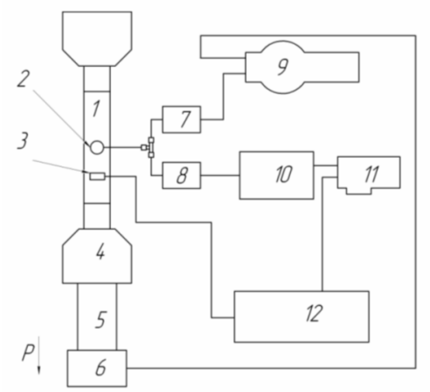

Fig. 15. Composite sample of test measuring aperture commutation scheme with longitude and transversal fibre orientation against loading vector direction:
1 — sample; 2 — AE sensor; 3 — strain gauge; 4 — gripper; 5 — hydro cylinder; 6 — dynamometer; 7, 8 — front amplifiers; 9 — PAC POCKET AE-2; 10 — AF-15; 11 — LCard L-783; 12 — strain gauge system

Chapter 4. Aviation Construction from Metallic Materials, Collapse Mechanism Research and Damage Assessment Using Acoustic Emission Method

4.1. The Study of Aviation Structure Metallic Material Collapse Mechanism Based on Airplane Shock Absorber Support Test Results

During chassis main support tests, brace-crane loop fatigue characteristics were studied [4,8,15,18] on shock absorber rod surface C — like a through fraction arise (Fig. 16).

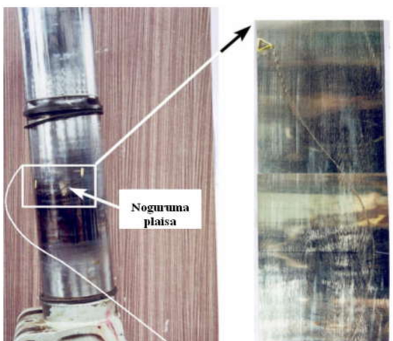

Fig. 16. Fraction on shock absorber rod

Fig. 17. Concentrator — cut (obtained after collapse)

The fraction is located on a rod surface phase with bottom cylinder axle box right where the site of oppression is. Contact traces of abrasion formed with many longitude grooves are located both on this phase of surface and axle box surface.

Due to high shock absorber rod collapse hazard in the operation conditions, this type of defect development observation and its identification opportunity studies were continued. For this purpose, shock absorber rod construction was artificially damaged — concentrator.

Concentrator shock absorber rod was inducted in the area where previous fatigue research led to a fatigue fracture. It was the kerf with length of 21 mm and with 8 mm (Fig. 17).

Since the usage of traditional non-destructive control methods without dissembling loop was limited, the AE method was used as the main method of fatigue fracture occurrence and development control. In parallel, periodic US control was performed every 200...400 loading cycles; to do this, trial was stopped and rod was pulled out from a shock absorber cylinder.

After 3550 loading cycle accusation shock absorption stem with the US control method fatigue fracture in size of 0.6...1.7 was found. In order to obtain overwhelming fatigue fracture were continued in the time of 1000 clocks (total actuation contained out of 4550 cycles) with US control every 200 loading blocs. Fracture assessment size after the end of tests was 0.2...1.8 mm. After the opening of fracture, it was found that fracture increased from both ends by 0.6...0.7 mm.

4.2. The Assessment Criteria of Metallic Material Fatigue Damage Based on Acoustic Emission Control

In a number of cases, α — criterion is used as material condition change criterion [9,10,16]. The proposed criterion is an angle between two lines which approximate to summary of AE changes in two existing phases next to it (Fig. 18). Most often, this criterion is used to indicate fraction occurrence and development. For example, Fig. 18 shows AE summary number N_{AE} depending on T with three marked α criteria, which represent the occurrence of three micro fractures. The use of this criterion is related to visual identification and it significantly depends on a chosen scale (which practically eliminates the possibility to standardise parameter and automate the control.)

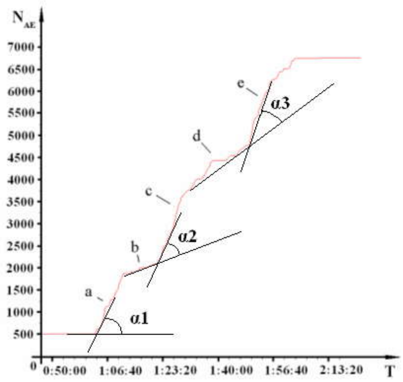

Fig. 18. AE summary number N_{AE} changes in the micro fracture formation process

As stated above, fatigue collapse has many stage characteristics. In this case, in the time of micro fracture occurrence, it can be determined in several ways: it is usually accompanied by a sharp summary AR or AE energy increase (there is such an effect if confirmed by fractographic studies). For this purpose, α — criterion can be used.

As for the further development of fracture, because of energy which is necessary for its development (compared to energy, which is consumed for micro fracture to appear), decay, α — criterion usage is ineffective. Partly, pre-collapse assessment problem can be solved, performing AE analyses in the cycle of load. Its work shows that if under different load cycles AR signal of micro and meso-fracture development stages varies one from another many times then moving to a macro fracture the difference significantly reduces (i.e., fracture development process stabilises).

Obviously, the best pre-collapse criteria could be created if the size of the fracture is known. However, because of the large energy difference in different stages of fracture, it is impossible to solve this problem in all the loading range. At the same time, if the fracture is observed after its initial creation (i.e., after a micro fracture stage), the energy relation in different stages significantly decreases, which can be used to determine the size of the fracture. Furthermore, instead of using fracture length, it is useful to use its open S area, which is more precisely related to the fracture energy. In this case, there is an opportunity to predict not only occurrence, but also development which is going under the fracture [3,11].

4.2.1. Damage Area Evaluation Criteria Based on the AE Measurement Data

The experimental data obtained during the test of the landing gear were used to evaluate the fatigue crack of the surface.

Based on formula 2.6 (Section 2.2), parameter A was expressed:

$$A = \frac{N_{AE2} - N_{AE1}}{(N_2 - N_1) \cdot P_{\max} \cdot S_{cr}} \left(\frac{imp.sk.}{cik \cdot kN \cdot mm^2}\right) \tag{4.1}$$

Based on the experimental results of the main chassis of MMA resources described in article [7], it was possible to calculate parameter A (Fig. 19):

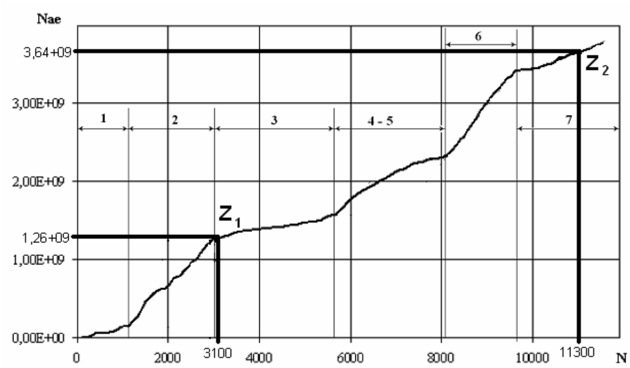

Fig. 19. AE Summary (N_{AE}) depending on the load cycle number (N):
1…7 — fracture development stages: $Z_n = (N_n, N_{AE\,n})$

$N_{AE1} = 1.26 \times 10^9$ (imp.sk.); $N_{AE2} = 3.64 \times 10^9$ (imp.sk.); $N_1 = 3.1 \times 10^3$ (cik);

$N_2 = 11.3 \times 10^3$ (cik); $P_{max} = 51.5$ (t); $S_{cr} = 50$ (mm^2).

Using these values in formula (4.1) the value A was determined:

$$A = 0.112 \left(\frac{imp.sk.}{cik \cdot kN \cdot mm^2}\right).$$

Considering parameter A, and knowing air screw pitch control lever experimental results described in article [13], the size of cracks S_{cr} by formula 2.6 was determined (Fig. 20):

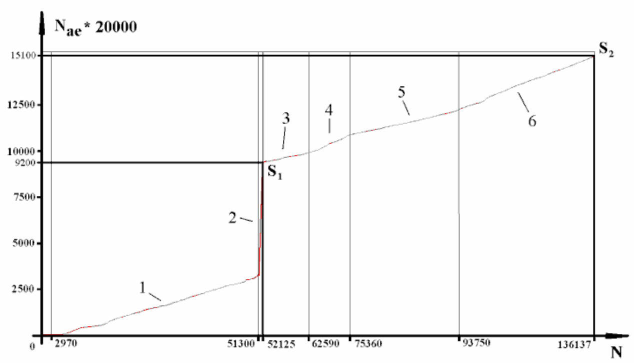

Fig. 20. AE Summary (N_{AE}) depending on the load cycle number (N):
1…6 — fracture development stages: $Z_n = (N_n, N_{AE\,n})$

$N_{AE1} = 18.4 \times 10^8$ (imp.sk.); $N_{AE2} = 30.2 \times 10^8$ (imp.sk.); $N_1 = 52125$ (cik);

N_2 = 136137 (cik); P_{max} = 46.2 (t).

It turned out that S_{cr} = 2.7 mm^2.

Measured fracture area consisted of 2.9 mm^2. The usage of proposed methods resulted in an error up to 6.9 %.

The obtained result showed sufficient tender affectivity.

4.2.2. Complex Criteria of Residual Construction Strength after Load Parameter

The methods and patents proposed in the present research are based on the following (Fig. 9.10) [2]:

1. The object has defect (in the considered chassis test example it is a fatigue fracture), which occurred in previous fatigue tests (or in previous operation).
2. Maintaining a normal load level defects virtually stop to develop (or develop very slowly); thus, in operation object collapse can happen after fixed resource to work (i.e., under casual operation conditions collapse does not happen).
3. Residual strength test load is gradually increased and at a certain loading level defect can quickly develop (if an object is in operation it can happen at load, which is greater than casual operation load or under special operation conditions)
4. During the test, load level and AE parameters are measured synchronously. In the beginning, defect development is accompanied by a stable AE growth summary.
5. The load is fixed at which this phenomenon occurs. The given load is as additional residual strength (strength limit or critical load) for object criteria which functioning with damages is limited or unacceptable (passenger transport, aerospace devices, nuclear energy devices, etc.).

Thus, the metallic material and construction fatigue assessment method is proposed, which is based on AE parameter measurements used to determine critical load (load limit) that corresponds to the beginning of catastrophic collapse. The method can be used to monitor acoustic emission constructions in aircraft operations.

Chapter 5. The Research of Aviation Composite Material Collapse Mechanism and Damage Assessment

5.1. Analyses of Aviation Composite Collapse Mechanism Based on Operation Data

This chapter provide KM mechanical properties and results of experimental reinforced collapse mechanism using the AE method. In studies reinforced plastic with anisotropic properties was used.

5.1.1. The Experimental Research on Composite Mechanical Collapse Using Acoustic Emission Measurement Data

Figure 21 shows different composite form and fibre orientation after test of collapse with static load.

According to experimental data measurement results of the processing results, AE parameter and graphic about load variation in time were built.

Part of samples was subjected to the testing during pre-loading in order to detect the effect on KM damage mechanisms and register AE signal characteristics (see Chapter 3). The initial summary AE (N_{AE}) of the time (T) dependence graph for a group of samples which was subjected to the initial loading, AE characteristics of parameter changes showed Kaiser effect, which was expressed as sudden AE radiating signal decrease in the time of re-loading to reach a previous load level. Since this range was not indicative to a loading condition, it was excluded from the further analysis (Fig. 22).

a)

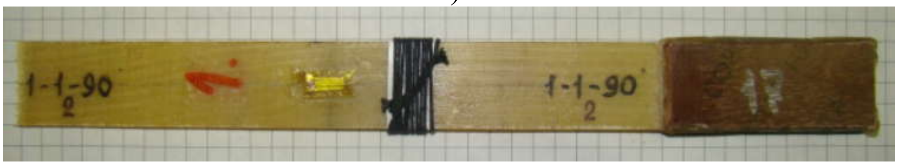

b)

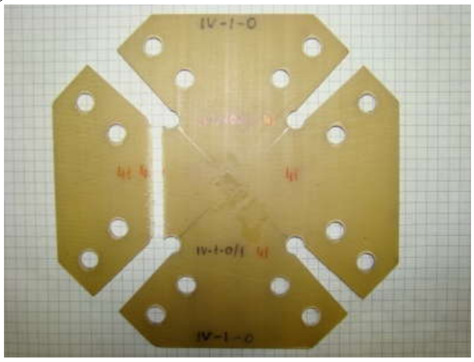

c) d)

Fig. 21. Appearance of experimental samples after tests:
a) Rectangular plate samples with longitudinal fibre orientation in relation to load vector in direction to the ends fixed in brackets; b) rectangular plate samples with a transversal fibre orientation in relation to the load vector direction with ends fixed in the brackets; c) cross-shaped sample; d) Maltese cross-shaped sample

The following connection data were obtained using AE hardware PAC POCKET AE-2. The data were obtained with equipment AF-15, the experimental connection had the same characteristics [21,22,23].

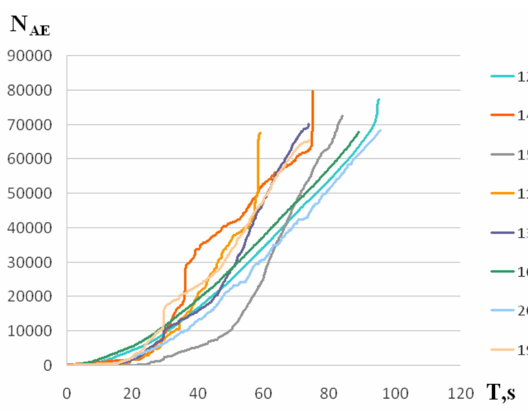

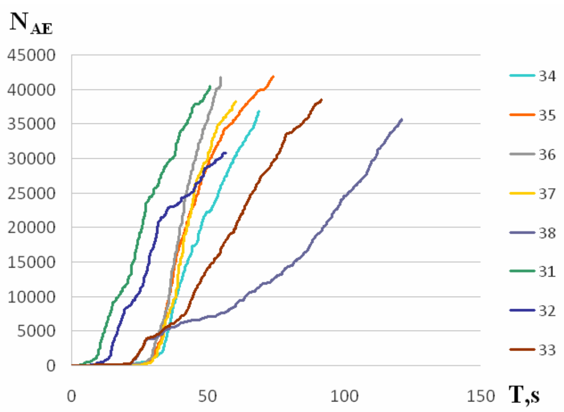

a) b)

Fig. 22. Corrected summary A (N_{AE}) of the time (T) dependence graph for a group of samples subjected to initial loading:
a) rectangular plate samples with longitudinal fibre orientation in relation to load vector in direction to the ends fixed in brackets; b) rectangular plate samples with a transversal fibre orientation in relation to the load vector in direction to the ends fixed in brackets

Test Results of Prototype not Subject to Preliminary Loading

Samples with Longitudinal Fibre Orientation in Relation to the Load Vector

AE signal amplitude value *Amp* depended on time *T* (Fig. 23) at the beginning of loading, and individual signals reached 63 dB (an average of 50 dB). When the load reached 66 % of the collapse value, individual signal amplitude reached 80 dB, but in the last stage of loading when the sample collapsed, it reached 100 dB.

The energy *E* depends on time *T* (Fig. 24), the value of the initial phase reached an average of 20 dB and practically did not change its value to 66 % of the collapse load. Reaching 66 % of the collapse value, energy began to rise sharply and reached 170 dB. AE signal energy value of sample collapse stage reached 1300 dB.

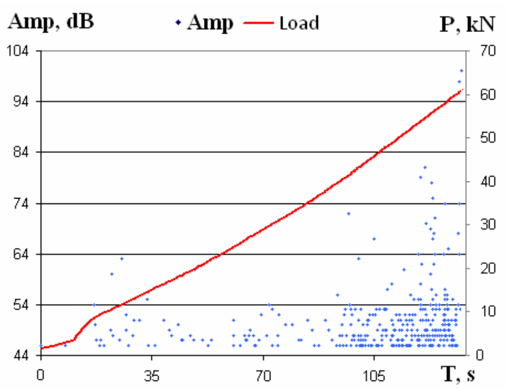

Fig. 23. AE signal amplitude (*Amp*) and load (*P*) changes in time (*T*)

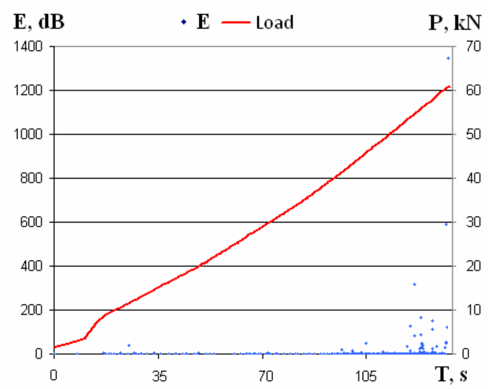

Fig. 24. AE signal energy (*E*) and pressure (*P*) changes in time (*T*)

The dependency of AE pulse amount *Hits* on the time *T* analyses (Fig. 25) showed a dramatic increase in the number of impulses from the moment of loading consisting of collapse load.

Summary of AE number N_{AE} depended on time *T* (Fig. 26), reaching the load limit that accounted for 66 % of the collapse load; a sudden N_{AE} increase was observed.

Fig. 25. Changes in AE impulse summary (*Hits*) and load (*P*) in time (*T*)

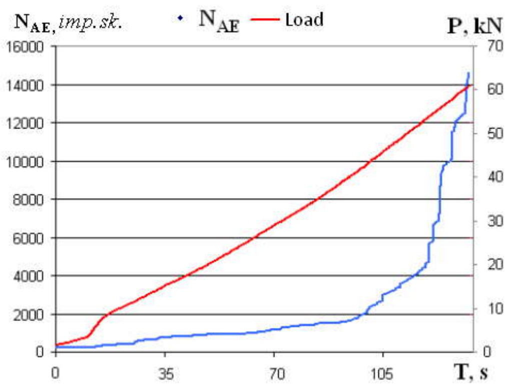

Fig. 26. Changes in summary AE number (N_{AE}) and load (*P*) in time (*T*)

At the same time, in the initial loading phase signal duration *Dur* (Fig. 27) increased from 100 µs to 200 µs. Reaching the level of load that accounted for 66 % of the collapse load, parameter *Dur* increased from 500 µs to 800 µs. AE signal length of collapses stage was equal to 2000 µs.

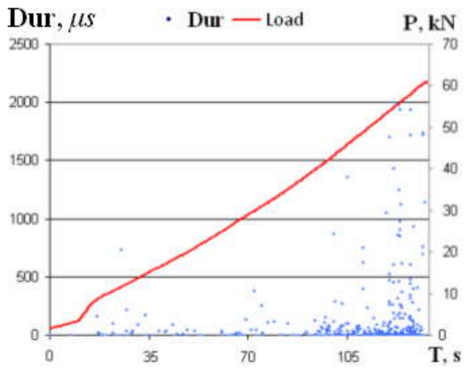

Fig. 27. Changes in signal duration (*Dur*) and load (*P*) in time (*T*)

5.1.2. KM Sample Analyses of Collapse Process

As revealed in the time of performed experiments, composite sample collapse nature depends on the location of fibre and the shape of sample.

Rectangular-shaped sample *with longitudinal fibre placement* is characterised by three phases of collapse: the first phase is connected with damage at the nano and micro level (up to 30 % of collapse load samples not subjected to previous loading (SPL) and respectively up to 30 % of the sample loaded previously (LP)) and continues with fracturing the matrix (up to 66 % of collapse load samples not subjected to SPL and up to 58 % of LP samples). The second phase is characterised by carrying fibre delamination, which end up with rapture — complete collapse of the sample (the third stage).

Rectangular-shaped sample *with transversal fibre placement* is characterised by three phases of collapse: the first phase is connected with damage at the nano and micro level (up to 30 % of collapse load samples not subjected to previous loading (SPL) and respectively up to 38 % of the sample loaded previously (LP)) and continues with fracturing the matrix (up to 74 % of collapse load samples not subjected to SPL and up to 61 % of LP samples). The second phase is characterised by carrying fibre delamination, which end up with rapture — complete collapse of the sample (the third stage).

Cross-shaped sample is characterised by three phases of collapse: the first phase is connected with damage at the nano and micro level (up to 45 % of collapse load samples not subjected to SPL and the LP ones), and continues with fracturing the matrix (up to 80 % of collapse load samples not subjected to SPL and up to 90 % of LP samples). The second phase is characterised by carrying fibre collapse number (most of the fibre was not damaged).

Maltese cross-shaped sample is characterised by three phases of collapse: the first phase is connected with damage at the nano and micro level (up to 48 % of collapse load samples not subjected to SPL and the LP ones), and continues with fracturing the matrix (up to 90 % of collapse load samples not subjected to SPL and up to 92 % of LP samples). The second phase is characterised by carrying fibre delamination, which end up with rapture — complete collapse of the sample (the third stage).

Analysing KM collapse borders (in the range of the first and second phases), it is visible that they are bigger on the rectangular samples with longitudinally and transversally located fibres not subjected to previous loading.

5.1.3. Static Analyses of Experimental Research Results

In order to evaluate the reliability of the results based on the known approaches, experimental data analyses were performed [27,29,30,31,32,33].

Based on the probabilistic approach, the following statistical characteristics were defined:

- average value ($\bar{X}$),
- static dispersion (S^2),
- average squared deviation (S),
- small selection average error (μ),
- small selection error boundary (Δ).

Taking into account that the author had a small number of samples (8 from every type of samples), for the statistical analyses small selection theory was used.

Small selection theory was developed by English statistician W. Gosset (operated under a pseudonym Student) at the beginning of the 20 century. In 1908, he developed a special selection, which allowed controlling small selections t and reliable probability *F(t)*. If $n > 100$, Student's selection table provides the same results as Laplace probability integral tables, at $30 \leq n \leq 100$ the differences are insignificant. Because of that, small selections are added to selections that have less than 30 items (a large selection is considered a selection with volume over 100 items).

Experimental data values are collected in EXCEL program and are shown in Appendix 1.

Statistical nature of the curves is shown in Appendix 2.

5.1.4. Overall Characteristics of the Obtained Results

As a result of experimental tests, a clear composite collapse process staging has been defined. AE parameter value clearly defines the stage of damage.

In all the cases, the initial loading phase is connected with damage in material at the nano and micro level, which is followed by fractures in the matrix. The second phase is connected with delamination of fibre and complete collapse of it.

The separate AE pulse value of the initial loading phase can reach a noticeable value, which is connected with the attrition processes in the securing device choosing the game. However, this signal is not connected with material damage to the mechanisms.

Composite matrix cracking process is followed by a signal with amplitude up to 75 dB; delamination phase is characterised by a signal amplitude value increase up to 85...95 dB, in the last phase, which takes place in the collapse of fibre, an amplitude value is in the range of 85 dB up to 100 dB. In the last two phases, there are AE signals with an amplitude value characteristic of crack, i.e., the processes happen at the same time.

The sample matrix collapse, delamination and fibre rapture are followed by AR signal intensity, duration and energy increase; furthermore, matrix collapse correspond to smaller intensity, duration and energy signal. AE signals at the moment of fibre collapse have maximum intensity, duration and energy than at the process of matrix collapse, but little less than at the process of fibre collapse.

Furthermore, AE signal energy changes describe the collapse process of fibre most accurately because the AE signal loading process initially has a short duration.

5.1.5. Material Damage Acoustic Emission Assessment

5.1.5.1. Acoustic Emission Evaluation Criteria of One Direction Oriented Composite Damage Level in Static Loading

The obtained summary number dependence of loading has equal AE summary number change characteristics for each test sample: slow AE growth stages are changed by a drastic change stage (Fig. 28). Several authors have discovered these regularities both for static loads and cyclical loads [28,36].

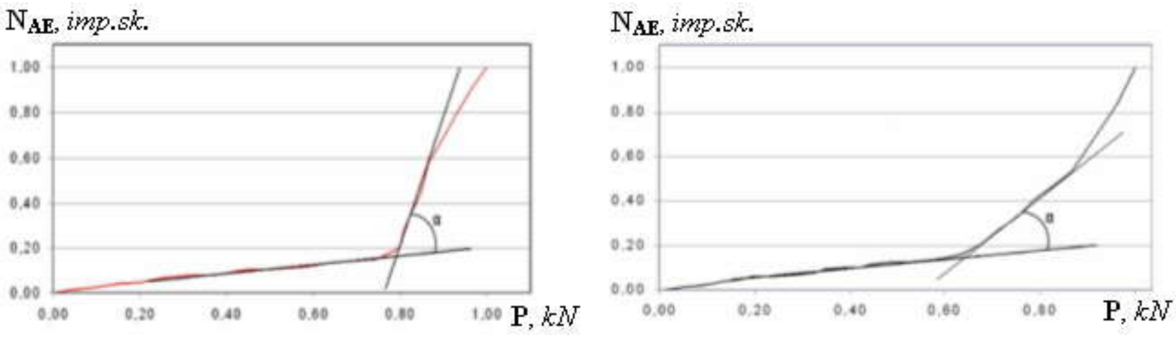

a) b)

Fig. 28. Summary number dependence on loading schedule relative value sample with angle α:
a) with transversal fibre positioning; b) with longitudinal fibre positioning crossing the initial loading

The mentioned stage crossings form angle α [22,23,28,36].

For the samples with longitudinal fibre orientation, this rapture begins in the range of 60 to 70 % (Fig. 29, a), which shows that fracturing in material takes place with the following delamination that concludes with carrying fibre collapse; as a result, the sample collapses.

For the samples with transversal fibre orientation, this rapture begins in the range of 60 to 75 % (Fig. 29, b), which shows that fracturing in material takes place with the following delamination that concludes with carrying fibre collapse; as a result, the sample collapses.

For the cross-shaped samples, this rapture begins in the range of 80 to 90 %, which shows that fracturing in material takes place with the following delamination that concludes with carrying fibre collapse; as a result, the sample collapses.

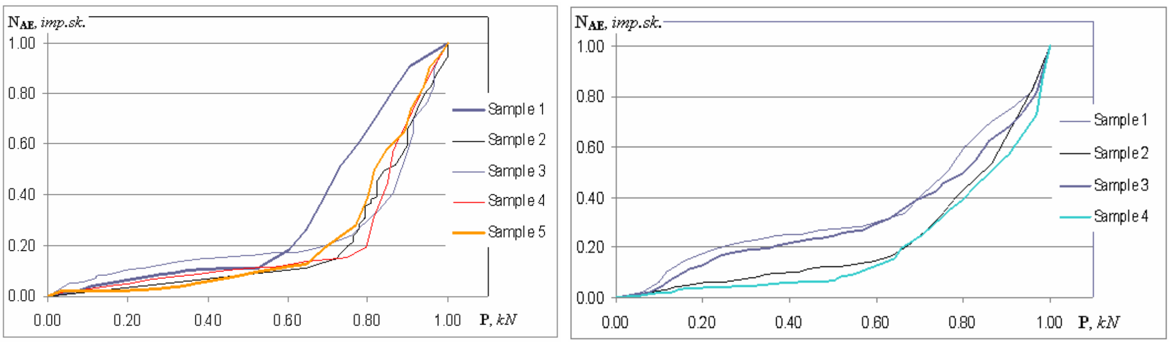

a) b)

Fig. 29. Summary number dependence of load schedule relative items:
a) sample with transversal fibre location: b) sample with longitudinal fibre location

Maltese cross-shaped sample rapture begins in the range of 90 %, which shows that fracturing in material takes place with the following delamination that concludes with carrying fibre collapse; as a result, the sample collapses.

The formation of angles characterises the beginning process of degradation, it remains until the collapse.

Thereby the acoustic emission method allows defining irreversible collapse beginning moment of one direction oriented composite.

5.1.5.2. KM Acoustic Emission Criteria of Collapse Intensity Evaluation

AE signal intensity (expressed as summary number (N_{AE}) changes depending on load (P)) is directly related to collapse intensity.

Figure 30 characterises this regularity conforming that at shorter angle α values the sample collapses at lover loads [21].

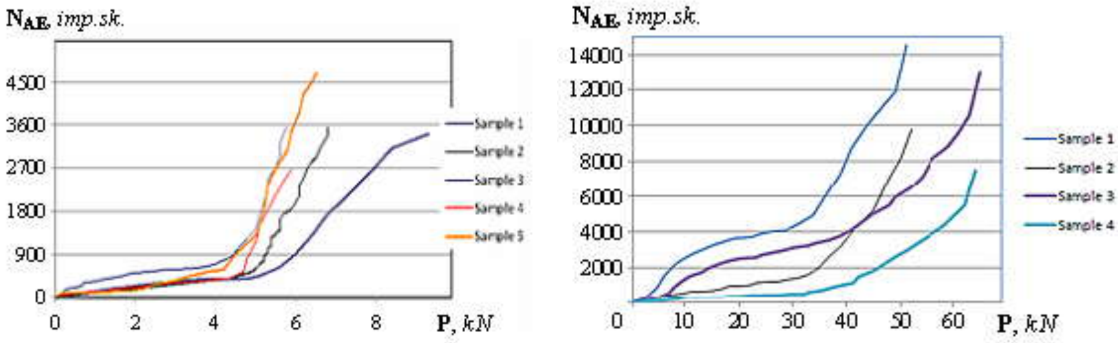

a) b)

Fig. 30. Summary number dependence on loading schedule:
a) sample with transversal fibre location; b) samples with longitudinal fibre location

5.1.5.3. Determination of Composite Construction Collapse Type by the Acoustic Emission Method

While performing the analyses of results, two main summary AE change relations were discovered (see Fig. 29 (a and b) in relative items) [1,11,12].

Given KM collapse characterisation the assessment method was developed.

When loads vector effect next to the fibre, smooth summary AE increase were observed (summary AR change gradient was changing and reached its maximum before collapse (Fig. 31, a).

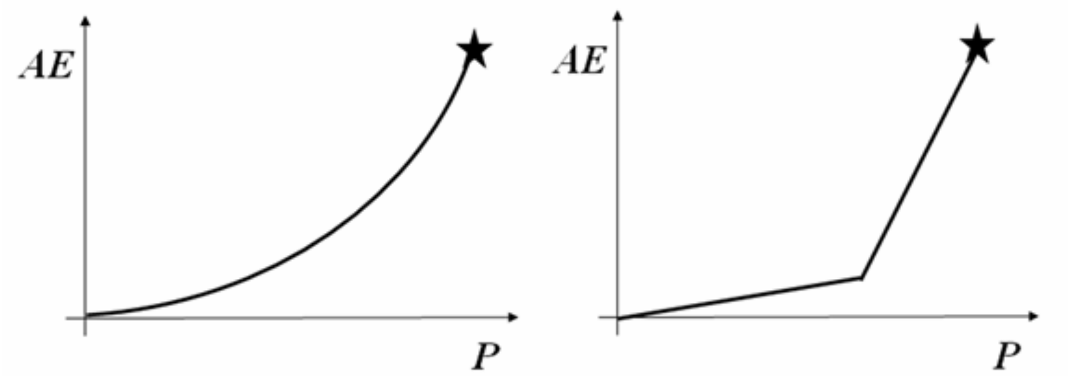

a) b)

Fig. 31. AE dependence of load:
a) mainly in the case of fibre collapse b) mainly in the case of matrix collapse

(★ - constriction collapse moment)

When the load vector affects perpendicularly the fibre direction, the load increases, and AE characteristics consisting of two phases are noticed (Fig. 31, b): in the first phase summary AE increases slowly, in the second — summary AE increases noticeably faster. The analyses of damage showed that delamination of material happened without collapse of carrying fibre. Thus, the summary AE change characteristics show composite matrix collapse.

5.2. Damage Assessment of Real Aviation Composite Construction

The collapse of aileron made of composite happened in the bottom panel by load P = 129 % (5070 kg) of collapse load P_p = 3668 kg, which corresponded to the load in hydro cylinder P_{HD} = 49.7 кN (5070 kg). Collapse was found in the model fastening area. Collapse view of aileron bottom panels is shown in Fig. 32, aileron front tip view is shown in Fig. 33.

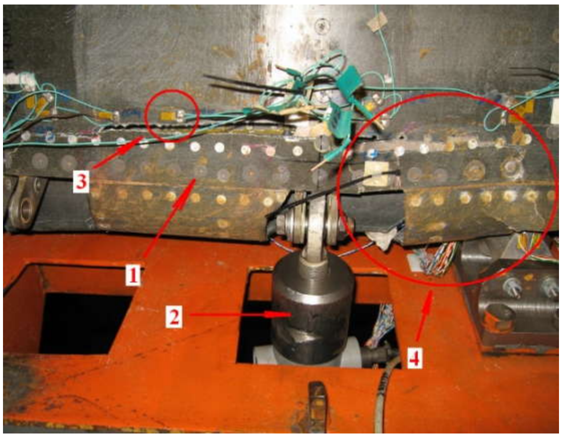

Fig. 32. Collapse of aileron bottom panels in the model booster area:
1 — aileron; 2 — booster; 3 — strain gauge giver; 4 — collapse area

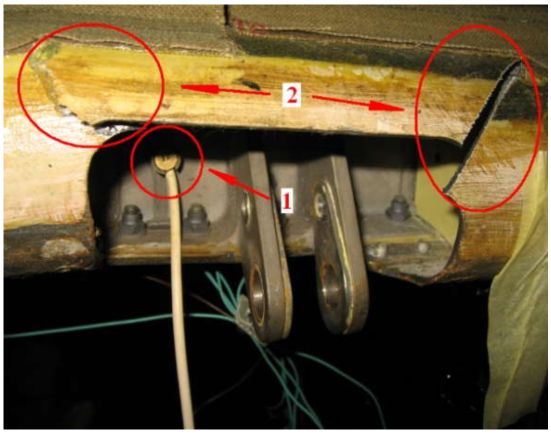

Fig. 33. Aileron nose collapse from top panel side piezo convert (AE giver) in the fastening area:
1 — AE giver; 2 — collapse area

Aileron collapse process can be described based on informative AE parameter analyses. Furthermore, likewise samples from KM aileron, the collapse process has 3 basic phases. For example, AE signal amplitude for separate collapse phases on average changed in the following way (Fig. 34): the first phase — up to 60 dB, the second one — up to 90 dB and the third phase — up to 100 dB.

The collapse process phase order is mainly characterised by AE signal energy changes in schedule by time (Fig. 35). In the first phase, energy value does not exceed 10 dB. In the second phase, energy value reaches 500 dB, in the third phase — up to 5000 dB.

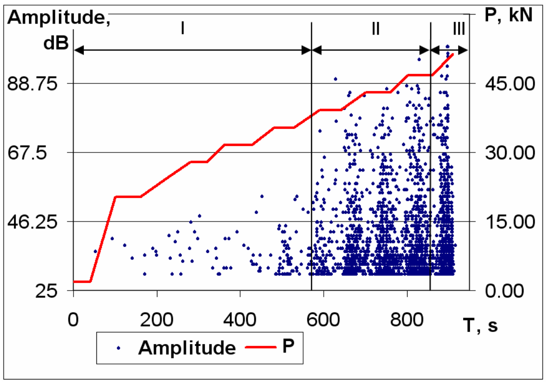

Fig. 34. AE signal amplitude (*Amp*) and load (*P*) changes in time (*T*)

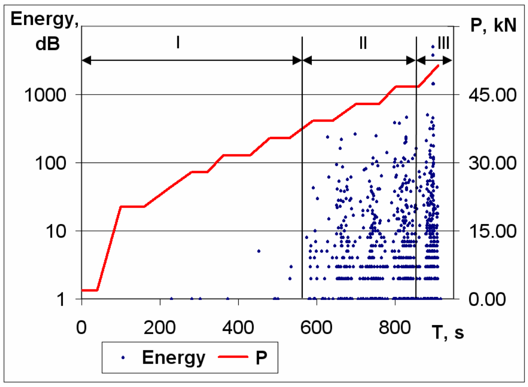

Fig. 35. AE signal energy (*E*) and pressure (*P*) changes in time (*T*)

Changes in impulse summary number and signal oscillation number in time, regularities are most accurately reflected in the construction collapse process in the second and third phases, which are KM fibre delamination and collapse (Figs. 36, 37, 38)

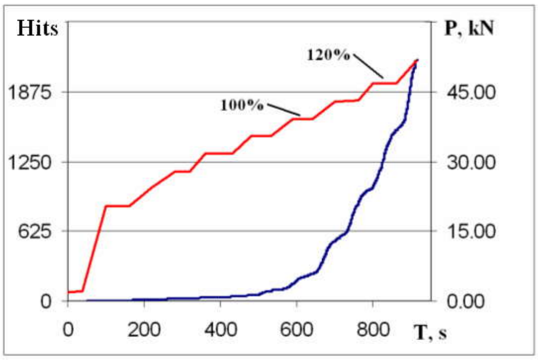

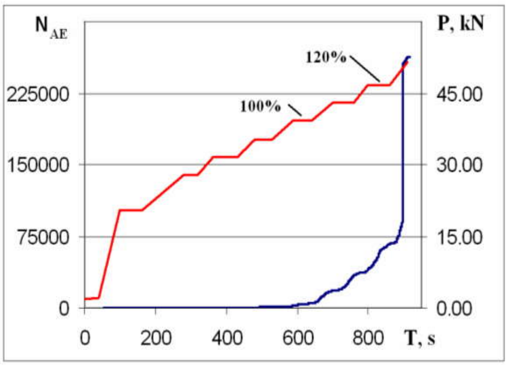

Fig. 36. Changes in AE impulse summary (*Hits*) and load (*P*) in time (*T*)

Fig. 37. Changes in summary AE number (N_{AE}) and load (*P*) in time (*T*)

From the obtained data (Figs. 36, 37, 38), it can be concluded that aileron construction intense collapse was observed in the phase up to 100 % of collapse load, but the following collapse process had catastrophic character until complete collapse which occurred reaching 129 % of collapse load.

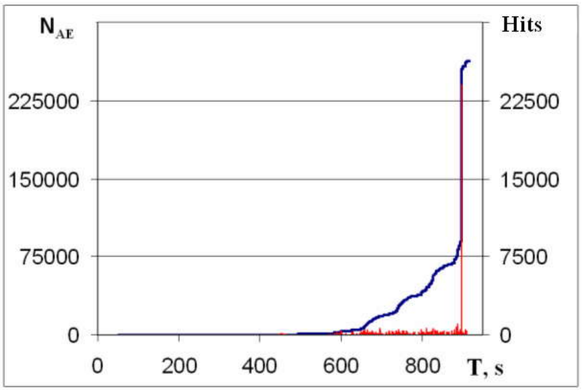

Fig. 38. Changes in summary AE number (N_{AE}) and AE impulse summary (*Hits*) in time (*T*).

Experimental data were obtained using real construction elements, confirmed damage evaluation criteria were obtained based on AE measurement data effectivity.

CONCLUSIONS

1) The assessment mathematical module of metallic material fatigue damage has been proposed based on acoustic emission signal measurement data under the condition of one cycle of loading in any stage of the damage. It has been shown that using AE parameter registration data, it is possible to assess the extent of material local plastic deformation, fatigue fracture length and area.
2) Damage mechanism of aviation constructions made of metallic material has been studied; as a result, new criteria for metallic fatigue damage assessment have been developed based on acoustic emission signal measurement control:
   a) Using the aircraft main landing chassis support and air prop pitch control lever, AE measurement (AE summary, imp.sk.*)* and test data (load size (kN), the number of load cycles (cik)), a new fatigue crack area size measurement method S_{cr} (damage area size, mm^2*)* has been used, which allows defining the area of the damage.

b) A new metallic material and construction fatigue resistant assessment method has been proposed, which is used to determine critical load that corresponds to the beginning of catastrophic construction collapse. Using AE measurement, as a result of the experiment, a possibility of finding critical load with a margin of safety of not less than 1.8 has been determined.

3) Different types of aviation composite collapse mechanisms under different load conditions and methods based on AE signal registration data have been studied. On the basis of experimental research, new composite damage degree assessment criteria have been developed, including:
   a) AE criteria that allow determining the beginning moment of irreversible collapse of one direction oriented composite;
   b) AE criteria that allow assessing composite collapse intensity;
   c) AE parameter that allows determining a composite collapse way, which means the detection of element that is crushed — fibre or matrix.
4) A real construction of composite collapse mechanism has been studied and its damage determination efficiency has been approved through the example of the aircraft wing ailerons using AE measurement data.

REFERENCES

1. *Doroško S., Harbuz Y. Kompozītmateriāla sagrūšanas tipa noteikšanas metode// LR Patents Nr. 14585. – 2012.*
2. *Harbuz Y., Doroško S. Maksimāli pieļaujamas slodzes noteikšanas paņēmiens izmēģinājumos uz paliekošo stiprību// Patents LV Nr. 14531. – 2012.*
3. *Harbuz Y., Doroško S. Plaisas lieluma noteikšanas paņēmiens noguruma pārbaudēs// LR Patents Nr. 14488. – 2012.*
4. *Nasibullins A. Akustiskās emisijas metodes pielietojuma izpēte aviotehnikas spēka konstrukciju kontrolei stendu izmēģinājumos. Promocijas darbs. – Rīga: RTU, 2011. – 137 lpp.*
5. *Urbahs A., Banovs M., Doroško S. Kuģa gāzturbīnu dzinēju kompresoru disku akustiskās emisijas kontrole// Maritime Transport and Infrastructure – 2010. – 2010. – 93.– 98. lpp.*
6. *Urbahs A., Banovs M., Doroško S., Fešcuks J. Kuģu gāzturbīnu iekārtu stāvokļa kontrole ar akustiskās emisijas metodi// Maritime transport and Infrastructure – 2009. – 2009. – 137.–141. lpp.*
7. *Urbahs A., Banovs M., Doroshko S., Nasibullins A., Turko V. Noguruma plaisu agrīnās atklāšanas tehnoloģija šasijas stenda izmēģinājumos// RTU zinātniskie raksti. – 2010. – Ser.6, Sēj.34. – 9.–16. lpp.*
8. *Banov M., Doroshko S., Nasibullin A., Turko V. Undercarriage fatigue test control by acoustic emission method// Ultragarsas. – 2006. – N2(59). – 16–18 p.*
9. *Banov M., Konyaev E., Troenkin D. Method of estimating the fatigue strength of turbine blades by acoustic emission// Fault detection. – 1981. – N2. – 26–28 p.*
10. *Banov M., Troenkin D., Urbahs A., Minatsevich S. Inspection of the condition of gas-turbine engine blades by the acoustic-emission method// The journal of nondestructive testing. – 1986. – 22(9). – 619–623 p.*
11. *Doroshko S., Harbuz Y. Acoustic emission analysis of fatigue crack development// Mechanika – 2012. – 2012. – 73–76 p.*
12. *Harbuz Y., Chepusov A. Methods of acoustic emission diagnostics of pre-destruction state// Transport means 2012. – 2012. – 228–231 p.*
13. *Nasibullin A., Harbuz Y., Doroshko S. Acoustic emission characteristics of fatigue crack development in a pitch control arm of helicopter lifting propeller blades// Transport Means – 2010. – 2010. – 49–52 p.*
14. *Shaniavski A. Modeling of Fatigue Cracking of Metals. Synergetics for Aviation. – Ufa: Publishing House of Scientific and Technical Literature "Monograph", 2007. – 500 p.*
15. *Shaniavski A., Urbahs A., Banov M., Doroshko S., Hodos N. Correlation of acoustic emission signals with kinetics of fatigue crack growth in the shock absorber of aircraft landing gear// Scientific Journal of Riga Technical University. – 2009. – V6, N31. – 94–100 p.*
16. *Troenkin D., Shaniavski A., Banov M., Konyaev E. Methodological recommendations for monitoring fatigue damage of low-dimensional structures using acoustic emission method. – M.: CSTI CA, 1985. – 52 p.*
17. *Urbahs A., Banov M., Doroshko S., Harbuz Y., Turko V. Acoustic Emission Diagnostic of Fatigue Crack Development During Undercarriage Bench Testing// Mechanika 2010. – 2010. – 450–454 p.*
18. *Urbahs A., Banov M., Doroshko S., Nasibullin A., Feshchuks Y. Acoustic emission monitoring of fatigue damage // High Tech in Latvia 2008. – Rīga: Latvia Technology Park, 2008. – 50 p.*

19. *Urbahs A., Banov M., Doroshko S., Turko V. Non-destructive inspection of aircraft landing gear during residual strenght testing// Ultragarsas=Ultrasound. – V64, N1. – 2009. – 43–45 p.*
20. *Urbahs A., Banov M., Harbuz Y., Chepusov A., Feshchuk Y. Evaluation of residual strength of aircraft aileron construction// AES – ATEMA 2011. – 2011. – 29–34 p.*
21. *Urbahs A., Banov M., Harbuz Y., Feshchuks Y., Sologubov Y. Evaluations of degree of damage and probability of forecasting of destructing load in anisotropic composites by means of acoustic emission in materials under static loading// Transport Means – 2011. – 2011.- 270–273 p.*
22. *Urbahs A., Banov M., Harbuz Y., Turko V., Feshchuk Y., Hodos N. Estimation of mechanical properties of the anisotropic reinforced plastics with application of the method of acoustic emission // Transport and Telecommunication. – 2010. – V11, N2. – 68–75 p.*
23. *Urbahs A., Banov M., Harbuz Y., Turko V., Feshchuk Y., Hodos N. Investigation of Mechanical Properties of Composite Materials Using the Method of Acoustic Emission// Mechanika – 2011. – 2011. – 306–310 p.*
24. *Urbahs A., Banov M., Turko V., Feshchuk Y. Diagnostics of Fatigue Damage of Gas Turbine Engine Blades// WASET Issue 59. – 2011. – Part IX. – 906–911 p.*
25. *Urbahs A., Harbuz Y., Urbaha J. Evaluating Of Damageability Of Materials At Fatigue Loading Based On Signals Of Acoustic Emission// Mechanika – 2015. – 2015. – p.*
26. *Urbahs A., Shaniavski A., Doroshko S., Banov M. Correlation of Acoustic Emission and Fractographic Characteristics during Fatigue Crack Development// EWGAE 2010. – 2010. – 1–8 p.*
27. *Архирейский А.А., Рассоха Е.Н. Статистическая обработка данных о надежности: Методические указания к выполнению расчетно-графической работы. – Оренбург: ГОУ, 2004. – 35 с.*
28. *Банов М.Д., Коняев Е.А., Троенкин Д.А. Методика оценки усталостной прочности газотурбинных лопаток методом акустической эмиссии. – М.: Дефектоскопия, 1981, №2. – 26–28 с.*
29. *Большев Л.Н., Смирнов Н.В. Таблицы математической статистики. – М.: Изд. “Наука”, 1983. – 415 с.*
30. *Веременюк В.В, Кожушко В.В., Мороз О.А. Статистическая обработка выборки значений случайной величины: Учеб. – метод. Пособие по высшей математике для студ. строит. спец. – Мн.: БГПА, 2002. – 102 с.*
31. *Гаскаров Д.В., Шаповалов В.И. Малая выборка. – М.: Статистика, 1978. – 248 с.*
32. *Иванова О.В., Дорофеева Н.С. Первичная обработка выборочных данных. Часть II: методические указания к лабораторному практикуму. – Томск: Изд-во Том. гос. архит.- строит. ун-та, 2012. – 35 с.*
33. *Кацман Ю.Я. Статистическая обработка эксперементальных данных: методические указания к лабораторным работам. – Томск: Изд-во Томского политехнического университета, 2008. – 38 с.*
34. *Качанов Л.М. Основы механики разрушения. – Москва: Наука, 1974. – 312 с.*
35. *Панасюк В.В., Андрейкив А.Е., Ковчик С.Е. Методы оценки трещиностойкости конструкционных материалов. – К.: Наукова думка, 1977. – 277 с.*
36 *Урбах А.И. Диагностика повреждений и прогнозирование разрушений авиационных конструкций акустико – эмиссионным методом. – Рига: РАУ, 1996. – 123 с.*